FGF2 Enhances Odontoblast Differentiation by αSMA+ Progenitors In Vivo

Vidović-Zdrilić, Ivana; Vining, K.H.; Vijaykumar, A.; Kalajzic, I.; Mooney, D.J.; Mina, M.

Source / Izvornik: **Journal of Dental Research, 2018, 97, 1170 - 1177**

Journal article, Published version
Rad u časopisu, Objavljena verzija rada (izdavačev PDF)

https://doi.org/10.1177/0022034518769827

Permanent link / Trajna poveznica: https://urn.nsk.hr/urn:nbn:hr:184:724808

FGF2 Enhances Odontoblast Differentiation by αSMA$^+$ Progenitors In Vivo

Journal of Dental Research
2018, Vol. 97(10) 1170–1177

DOI: 10.1177/0022034518769827
journals.sagepub.com/home/jdr

I. Vidovic-Zdrilic[1], K.H. Vining[2], A. Vijaykumar[1], I. Kalajzic[3], D.J. Mooney[2], and M. Mina[1]

Abstract

The goal of this study was to examine the effects of early and limited exposure of perivascular cells expressing α (αSMA) to fibroblast growth factor 2 (FGF2) in vivo. We performed in vivo fate mapping by inducible Cre-loxP and experimental pulp injury in molars to induce reparative dentinogenesis. Our results demonstrate that early delivery of exogenous FGF2 to exposed pulp led to proliferative expansion of αSMA-tdTomato$^+$ cells and their accelerated differentiation into odontoblasts. In vivo lineage-tracing experiments showed that the calcified bridge/reparative dentin in FGF2-treated pulps were lined with an increased number of *Dspp*$^+$ odontoblasts and devoid of *BSP*$^+$ osteoblasts. The increased number of odontoblasts derived from αSMA-tdTomato$^+$ cells and the formation of reparative dentin devoid of osteoblasts provide in vivo evidence for the stimulatory effects of FGF signaling on odontoblast differentiation from early progenitors in dental pulp.

Keywords: reparative dentinogenesis, pulp biology, stem cells, perivascular cells, dentin matrix protein 1 (DMP1), dentin sialophosphoprotein (DSPP)

Introduction

The dentin-pulp complex has a regenerative potential leading to the formation of tertiary dentin. Mild stimuli lead to reactionary dentinogenesis, during which preexisting odontoblasts upregulate their secretory activity (Sloan and Smith 2007; Sloan and Waddington 2009). However, trauma of greater intensity that causes the death of the preexisting odontoblasts leads to reparative dentinogenesis involving the recruitment and proliferation of progenitor cells to the site of injury and their differentiation into a second-generation of odontoblasts or "odontoblast-like cells" (Sloan and Smith 2007; Sloan and Waddington 2009). These odontoblast-like cells synthesize a dentin-like mineralized tissue, the reparative dentin also referred to as osteodentin, immediately below the site of damage to preserve pulp vitality (Tziafas 2004; Sloan and Smith 2007; Sloan and Waddington 2009).

Genetic lineage tracing in continuously growing incisors of adult mice showed the contribution of several distinct populations of mesenchymal stem cells (MSCs) including peripheral nerve-associated glial cells, periarterial Gli1-expressing cells, and NG2-expressing pericytes (Feng et al. 2011; Kaukua et al. 2014; Zhao et al. 2014) to reparative dentinogenesis. Our recent lineage-tracing study in adult mice molars showed the major contribution of resident perivascular cells expressing α smooth muscle actin (αSMA) to reparative dentinogenesis (Vidovic et al. 2017).

Reparative dentinogenesis is dependent on multiple signaling molecules, sequestrated in the dentin matrix and pulp supportive tissues (Tziafas 2004; Sloan and Smith 2007; Sloan and Waddington 2009). These signaling factors are involved in many aspects of healing and repair including neovascularization, proliferation, migration of progenitor cells to the site of injury, and their differentiation into a second-generation of odontoblasts expressing high levels of dentin sialophosphoprotein (DSPP; Tziafas 2004; Sloan and Smith 2007; Sloan and Waddington 2009).

Our recent in vitro studies showed roles and contributions of fibroblast growth factors (FGFs) on reparative dentinogenesis (Sagomonyants and Mina 2014; Sagomonyants et al. 2015, 2017). The effects of FGF2 on differentiation of pulp cells into odontoblasts are stage specific and depend on the stage of cell maturity (Sagomonyants and Mina 2014; Sagomonyants et al. 2015, 2017). FGF2 inhibited the terminal differentiation and expression of *Dspp* in more mature populations of functional odontoblasts (Sagomonyants et al. 2017). Conversely, FGF2 accelerated the differentiation and increased

[1]Departments of Craniofacial Sciences, School of Dental Medicine, University of Connecticut Health Center, Farmington, CT, USA
[2]John A. Paulson School of Engineering and Applied Sciences and Wyss Institute for Biologically Inspired Engineering, Harvard University, Cambridge, MA, USA
[3]Departments of Reconstructive Sciences, School of Dental Medicine, University of Connecticut Health Center, Farmington, CT, USA

A supplemental appendix to this article is available online.

Corresponding Author:
M. Mina, Division of Pediatric Dentistry, Department of Craniofacial Sciences, School of Dental Medicine, University of Connecticut Health Center, 260 Farmington Ave, Farmington, CT 06030, USA.
Email: Mina@uchc.edu

numbers of differentiated odontoblasts expressing *Dspp* from early progenitors (Sagomonyants et al. 2015). These observations showed that early and limited exposure of pulp cells to FGF2 alone promotes odontoblast differentiation and provided critical insight for the development of improved treatments for vital pulp therapy and dentin regeneration (Sagomonyants et al. 2015).

The purpose of this study was to gain further insight into the response of the perivascular cells expressing αSMACre-tdTomato (Vidovic et al. 2017) to early and limited exposure to FGF2 in vivo using cell lineage tracing in the mice molars.

Materials and Methods

Animal Models

αSMACreERT2/Ai9, αSMA-GFP, and Col2.3-GFP mice used in this study have been previously described (Vidovic et al. 2017). For in vivo lineage-tracing experiments,αSMACreERT2/Ai9; Col2.3-GFP (cross between αSMACreERT2/Ai9 with Col2.3-GFP mice) were used (Roguljic et al. 2013). Animal protocols were approved by the Institutional Animal Care Committee. In lineage-tracing studies, 4-wk-old mice were injected intraperitoneally (i.p.) with corn oil (vehicle [VH]) or tamoxifen (TM; 75 μg/g body weight) twice in 24-h intervals. The untreated, VH-injected αSMACreERT2 mice and αSMA CreERT2^{negative}/Ai9 TM-treated mice were examined as controls for spontaneous Cre activation in pulp tissue in vivo.

Experimental Pulp Injury

Two days after the second TM injection, experimental pulp exposures on the occlusal surface of the maxillary first molars were prepared as described (Vidovic et al. 2017). After exposures, bleeding was controlled with sterile paper points and saline, and FGF- and VH-soaked beads were placed on the site of exposure. Pulps were sealed with mineral trioxide aggregate (MTA) and light-cured composite resin as described before (Vidovic et al. 2017).

Preparation of Beads

Beads (BIO-RAD Affi-Gel Blue Gel, 100- to 200-μm diameter) were washed with phosphate-buffered saline (PBS) and soaked in solution containing 10ng/μL of recombinant FGF2 (R&D) or 0.1% bovine serum albumin (BSA; control) and incubated at 37°C for 30 min. Protein-soaked beads were used right after incubation.

Release Profile of FGF2 from Beads

Beads were hydrated in 10 ng/μL of FGF2 in PBS to load beads with FGF2. Beads were then transferred to low-binding 1.5-mL tubes and centrifuged at 300*g* for 1 min. Supernatant was discarded and replaced with 1 mL aMEM release media (1% heat-inactivated BSA). Cumulative release of FGF2 was measured by collecting 1 mL of conditioned media at each time point and replacing with fresh media. The dry mass of beads was determined after the last time point by transferring to distilled water in a 1.5-mL tube with recorded mass, centrifuging to remove water, and desiccating overnight. The amount of FGF2 released into the media was measured by enzyme-linked immunosorbent assay (R&D). Release of FGF2 was normalized to the mass of beads in each condition.

Histological Analysis

Animals were sacrificed with CO_2 at various time points (2, 7, 14 d and 4 wk). Maxillary arches were dissected, fixed, decalcified, and embedded in cryomatrix (Thermo Shandon) as described before (Frozoni et al. 2012; Vidovic et al. 2017). Seven-micrometer sections were obtained using the Leica cryostat and mounted using a CryoJane tape transfer system (Instrumedics). Sections were examined and imaged using a Zeiss microscope and filter cubes optimized for GFP and Td-Tomato variants. Adjacent sections were processed for hematoxylin and analyzed by light microscopy.

For analysis of the fate of αSMA-tdTomato^{+} and Col2.3^{+} cells, all sections through the site of injury and repair (at least 7 to 15 sections per tooth) were evaluated at each time point. At each time point, the percentage of areas of red-labeled and yellow-labeled (double-labeled) cells in defined areas of the pulp chambers in intact and injured teeth were calculated using ImageJ software. Results represent mean and ±SEM in 3 to 6 independent experiments; $P \leq 0.05$ relative to control at each time point.

Primary Cultures, Gene Expression, and Flow Cytometric Analysis (FACS Analysis)

Primary cultures of dental pulp were prepared from P5-P7 αSMA-GFP as described previously (Balic et al. 2010). Three days after initiation of cultures, 20 ng/mL FGF2 or 0.1% BSA (control) was added to the media. At day 7, when cells reached confluence, cultures were grown in mineralization-inducing medium containing 50 μg/mL of fresh ascorbic acid and 4 mM β-glycerolphosphate without FGF2 for additional 10 d. Media were changed every alternate day. At various time points, total RNA was isolated using TRIzol reagents (Invitrogen), followed by cDNA synthesis. Gene expression was examined by TaqMan quantitative polymerase chain reaction analyses using the primers and conditions as previously described (Sagomonyants et al. 2015).

For fluorescence-activated cell sorting (FACS) analysis, BSA- and FGF2-treated cultures were processed at 24, 48, 72, and 96 h after treatment. For staining with EdU (5-ethynyl-2′-deoxyuridine), cells were treated with 10 μM EdU for 4 h and detached by mild trypsin/EDTA (Invitrogen) digestion followed by centrifugation at 4 °C. Cells were processed for staining using Click-iT Plus Flow Cytometry Assay kit (Invitrogen) according to the manufacturer's instructions. After staining, cells were washed in 1%BSA in PBS, resuspended in 300 to 400 μL of FACS medium, and strained through a 70-μm

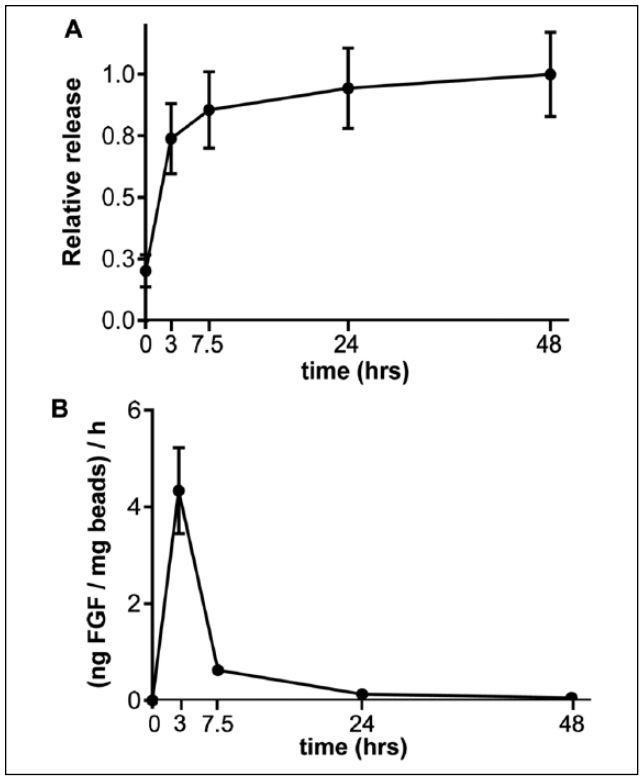

Figure 1. Release of fibroblast growth factor (FGF) from heparin beads. (**A**) Relative cumulative release of FGF from agarose beads, normalized by mass of heparin beads, showing that 90% of FGF release is achieved over the first 10 h. (**B**) Absolute rate of release of FGF (ng FGF per mg beads) per hour, showing that the peak release rate occurs in the first 3 h and then dramatically reduces to zero over 48 h. Results represent mean ± SEM of enzyme-linked immunosorbent assay measurements in 6 independent experiments.

strainer to obtain single-cell suspension. Approximately 50 000 to 100 000 cells/sample were collected by a BD LSR-II FACS cytometer (BD Biosciences). Pulp cells from nontransgenic littermates served as a negative control for GFP transgene expression in all experiments. Pulp cells from nontransgenic littermates and cells not stained with primary antibody served as controls.

Fluorochrome Labeling of Mineralizing Tissue. The dynamic process of mineral apposition in newly formed reparative dentin was examined after weekly i.p. injection of fluorescent dyes dissolved in 2% $NaHCO_3$ (pH = 7.4). These injections started 1 wk after pulp exposure and included calcein green (6 mg/ kg), demeclocycline (60 mg/kg), and alizarin complexone (30 mg/kg; Sigma-Aldrich). Animals were sacrificed by intracardiac perfusion and processed for histology 1 d after the injection of last dye.

RNAscope In Situ Hybridization

RNAscope in situ hybridization was conducted using RNAscope BROWN kit for *Dspp* and *Bsp*, according to the manufacturer's instructions (Advanced Cell Diagnostics).

Statistical Analysis of Data

Results represent mean ± SEM of at least 3 independent experiments. Statistical analysis was performed by GraphPad Prism 6 software using Student's *t* test. Statistical significance was determined at $P \leq 0.05$.

Results

Characterization of Release Profile of FGF2 from Beads

Agarose beads were used as a carrier for release of FGF2. An in vitro release assay showed that approximately 90% of FGF2 was released from beads into culture media during the first 10 h (Fig. 1A). The release rate of FGF2 (ng FGF2/mg beads/h) peaked in the first 3 h, followed by a marked decrease over the subsequent 45 h (Fig. 1B).

Early Response of αSMA-tdTomato$^+$ Cells to FGF2

Using previously characterized αSMACreERT2/Ai9;Col2.3-GFP transgenic mice and lineage tracing, we examined the effects of limited FGF2 released from beads on the activation of αSMA-tdTomato$^+$ cells after experimental pulp exposures. In these experiments, 4-wk-old αSMACreERT2/Ai9;Col2.3-GFP transgenic animals were first injected with TM and VH (twice, 24-h interval) followed by experimental pulp exposures and application of beads soaked in BSA (control) and FGF2 to the exposed pulp tissue. The absence of Col2.3-GFP$^+$ odontoblasts after experimental pulp exposures (Fig. 2B) confirmed adequate removal of dentin and destruction of odontoblasts, which are essential for the initiation of reparative dentinogenesis. The specificity of Cre activation was examined by the absence of αSMA-tdTomato$^+$ in pulps and surrounding tissues in VH-injected animals with and without pulp exposures (Appendix Fig. 1A).

Sections from control (uninjured/intact) first maxillary molars from the TM-injected animals 2 d postinjection showed a few αSMA-tdTomato$^+$ cells in dental pulp and in bone marrow of alveolar bone (Appendix Fig. 1B), which increased thereafter. In these locations, αSMA-tdTomato$^+$ cells were detected in close proximity to CD31$^+$ cells, as previously reported (Vidovic et al. 2017).

Pulp injury and application of beads soaked in BSA and FGF2 resulted in the activation and expansion of αSMA-tdTomato$^+$ cellsin the pulp as early as 2 d (Fig. 2C, D) as compared with intact uninjured teeth (Appendix Fig. 1B). Activation and expansion of αSMA-tdTomato$^+$ was detected in areas in close vicinity as well as at a distance from the site of injury (Fig. 2). Between 2 and 14 d after pulp exposures, αSMA-tdTomato$^+$ cells expanded, migrated, and arrived at the sites of injury in both BSA- and FGF-treated pulps (Fig. 2C, D). The area occupied by αSMA-tdTomato$^+$ cells in the coronal pulp chambers of FGF2-treated pulps at 2 and 7 d after pulp exposure was greater than that in BSA-treated pulps (Fig. 3B).

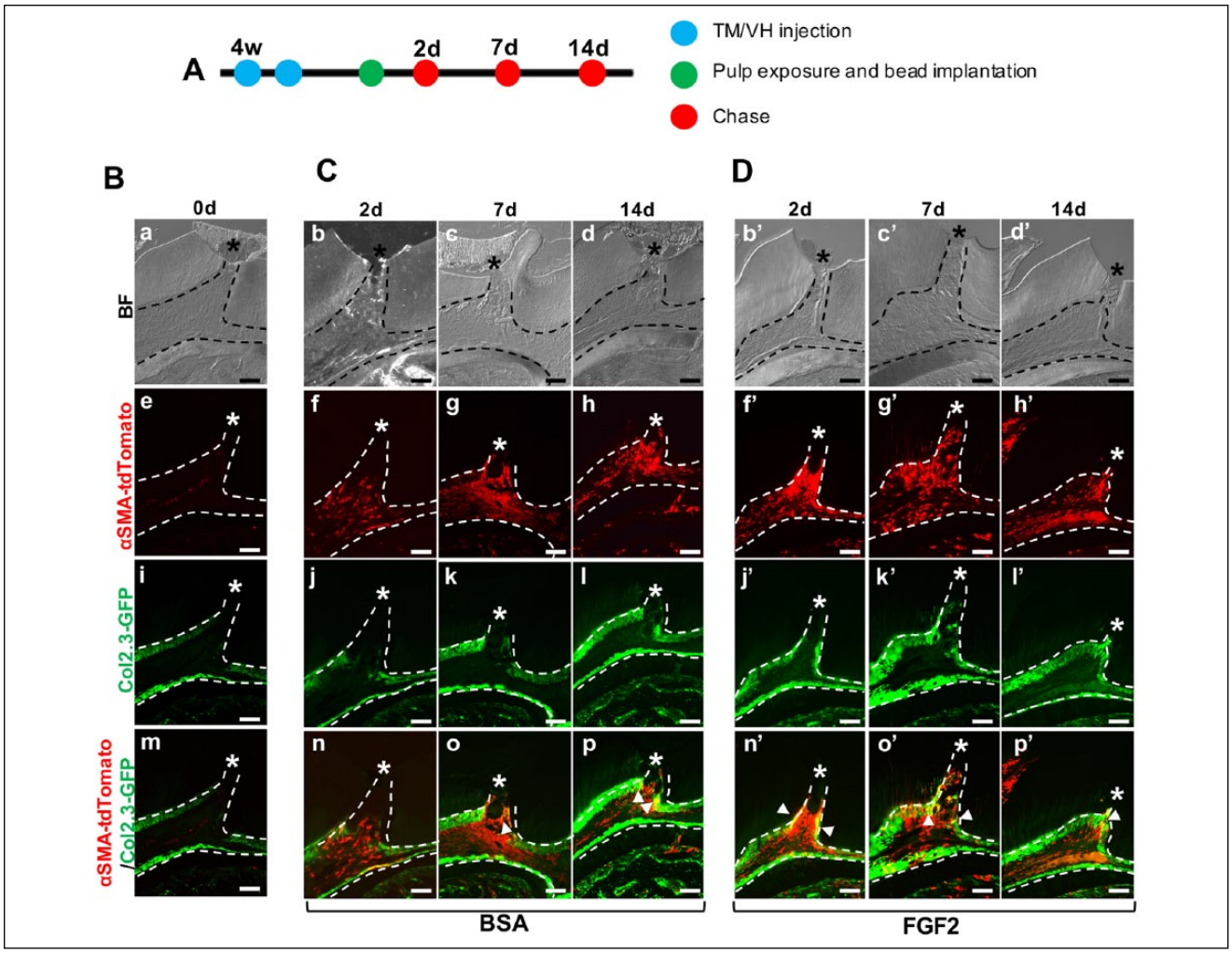

Figure 2. Early response of αSMA-tdTomato$^+$ cells to fibroblast growth factor 2 (FGF2) after pulp exposure. (**A**) Scheme of lineage-tracing experiments in αSMACreERT2/Ai9;Col2.3-GFP during reparative dentinogenesis. Four-week-old animals were injected with tamoxifen (TM) twice within a 24-h interval. Pulp exposures were performed 48 h after the second injection. Beads were placed on the exposed pulps, and animals were chased at indicated time points after pulp exposure and bead implantation. (**B**) Bright field (a) and epifluorescence (e, l, m) images of sagittal sections through a maxillary first molar immediately after pulp exposure. Note the presence of a few αSMA-tdTomato$^+$ cells in the center of pulp chamber (e) and the lack of 2.3-GFP$^+$ cells (i) and double-labeled cells (m) at the site of exposure. (**C**) Bright field (b–d) and epifluorescence (f–p) images of sagittal sections through BSA-treated maxillary first molars at indicated time points. (**D**) Bright field (b′–d′) and epifluorescence (f′–p′) images of sagittal sections through FGF-treated maxillary first molars at indicated time points. Note the continuous increases in number of αSMA-tdTomato$^+$ cells in both BSA- and FGF2-treated teeth over time. In both BSA- and FGF-treated teeth, αSMA-tdTomato$^+$ cells arrived at the site of exposure. Note the appearance of Col2.3-GFP$^+$ cells with time at the site of injury in both BSA- and FGF-treated teeth. Also note that in the BSA-treated tooth, cells coexpressing both αSMA-tdTomato and Col2.3-GFP transgenes (yellow, indicated by arrowheads) in close proximity to the site of injury are not detected at 2 d (n) but are detected at 7 and 14 d (o and p). In FGF2-treated teeth, cells coexpressing both transgenes are detected as early as 2 d (n′) with increases at 7 and 14 d (o′–p′). In all images, dental pulp is denoted by dashed lines and the site of pulp exposure by an asterisk. Scale bars = 100 μm.

Effects of FGF2 on Proliferation of αSMA-tdTomato$^+$ Cells

To examine the underlying mechanisms of increases in the number of αSMA-tdTomato$^+$ cells in the pulp chamber by FGF2, the effect of FGF2 on proliferation was examined by staining with EdU, a nucleoside analog to thymidine that is incorporated into DNA primarily during the S phase. Flow cytometric analysis showed marked and clear increases in the percentage of αSMA-GFP$^+$, EdU$^+$, and αSMA-GFP$^+$/EdU$^+$ cells in FGF2-treated cells as compared with BSA-treated cultures (Table A–C). These results indicated that FGF2 has proliferative effectson pulp cells expressing αSMA.

Effects of FGF2 on the Differentiation of αSMA-tdTomato$^+$Cells

Next, we examined the effects of FGF2-soaked beads on the fate and differentiated progenies of αSMA-tdTomato–derived cells in vivo by examining the time of appearance and the percentage of cells coexpressing both αSMA-tdTomato and Col2.3-GFP transgene. This transgene has been previously

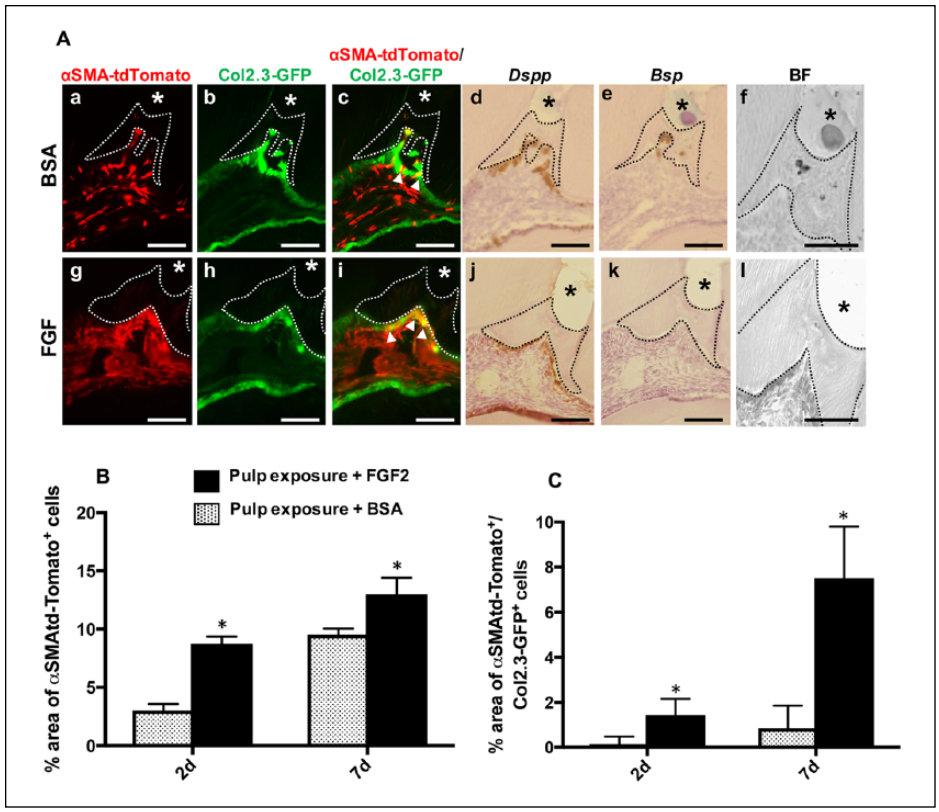

Figure 3. Fibroblast growth factor 2 (FGF2) induced differentiation of αSMA-tdTomato$^+$ cells. (**A**) Representative epifluorescence (a–c) images of sections through maxillary molars of αSMACreERT2/Ai9;Col2.3-GFP animals 4 wk after implantation of bovine serum albumin (BSA) beads. Adjacent sections were processed for RNAscope in situ hybridization for *Dspp* (d) and *Bsp* (e). Higher magnification, bright field image (f) showing the mineralized tissue underneath the site of injury in a BSA-treated tooth. Representative epifluorescence (g–i) images of sections through maxillary molars of αSMACreERT2/Ai9;Col2.3-GFP animals 4 wk after implantation of FGF2 beads. Adjacent sections were processed for RNAscope in situ hybridization for *Dspp* (j) and *Bsp* (k). Higher magnification, bright field image (l) showing the mineralized tissue underneath the site of injury in an FGF2-treated tooth.The mineralized tissue at the site of injury in a BSA-treated tooth is disorganized and unlike adjacent dentin (f). On the other hand, in the FGF2-treated tooth, the mineralized tissue at the site of injury appears organized and more similar to adjacent dentin (l). In all images, mineralized tissue at the site of injury is denoted by dashed lines and the site of pulp exposure by an asterisk. Scale bars = 100μm. **B** and **C** are histograms showing the changes in the percentage of areas occupied by αSMA-tdTomato$^+$ (B) and αSMA-tdTomato$^+$/Col2.3-GFP$^+$ (C) in pulp chambers of BSA- and FGF2-treated maxillary molars 2 and 7 d after pulp exposure. Note the significant increases in the percentage of αSMA-tdTomato$^+$ and αSMA-tdTomato$^+$/Col2.3-GFP$^+$ areas in pulp chambers of FGF2-treated teeth as compared with BSA-treated teeth. Results represent mean and ±SEM in 3 to 6 independent experiments; $P \leq 0.05$ relative to control at each time point.

shown to be expressed by both odontoblasts and osteoblasts (Braut et al. 2003).

Histological analysis showed that in BSA-treated teeth, a few cells coexpressing both transgenes were detected at 14 d but not at 2 and 7 d (Fig. 2C n–p). In FGF2-treated teeth, double-labeled cells were detected as early as day 2 and increased thereafter (Fig. 2D n′–p′). The area occupied by double-labeled cells in the coronal pulp chambers in FGF2-treated teeth was larger than that in BSA-treated teeth (Fig. 3C).

The formation of calcified bridge/reparative dentin lined with double-labeled cells in both FGF-and BSA-treated teeth was detected 4 wk after the pulp exposure (Fig. 3A). Using fluorochrome mineral labeling, we previous showed the deposition of a new calcified matrix at the site of injury and reparative dentinogenesis (Vidovic et al. 2017). To ensure that calcified bridge/reparative dentin in FGF2-treated pulp also resulted from the deposition of new calcified matrix, we performed fluorochrome mineral labeling at different time points (Appendix Fig. 2A). Histological examination of molars 4 wk after pulp exposure showed 3 distinct labeled lines in the calcified bridge/reparative dentin formed at the site of injury in FGF2-treated pulps (Appendix Fig. 2A), indicating the formation of new mineralized matrix. There was an increased number of double-labeled cells lining the calcified bridge in FGF2-treated teeth (Fig. 3Ai) compared with BSA-treated teeth (Fig. 3Ac).

The phenotype of the double-labeled cells lining the calcified bridge was further examined by RNA scope in situ hybridization using probes for *Bsp* and *Dspp*, which are markers for differentiated osteoblasts and odontoblasts, respectively (Appendix Fig. 1C). In BSA-treated teeth, both *Dspp*$^+$and *Bsp*$^+$cells were detected in double-labeled cells lining the newly formed calcified bridge/reparative dentin (Fig. 3 Ad, Ae). The formation of both *Dspp*$^+$ and *Bsp*$^+$ cells from αSMA-tdTomato$^+$ cells was consistent with our previous studies indicating the formation of osteodentin immediately below the site of injury (Vidovic et al. 2017). On the other hand, double-labeled cells lining the calcified bridge in FGF2-treated teeth displayed only *Dspp*$^+$ cells and not *Bsp*$^+$ cells (Fig. 3Aj, 4Ak). Examination of sections 4 wk after pulp exposure also showed that activated αSMA-tdTomato$^+$ cells at a distance from the site of injury give rise to pulp cells (Appendix Fig. 2B).

The FGF2-induced changes in the gene expression were further examined in primary dental pulp cultures. Limited and early treatment of these cultures with FGF2 resulted in earlier and increased expression of *Dspp* as compared with BSA-treated cultures (Fig. 4A). In FGF2-treated cultures, the relative levels of *Bsp* were significantly reduced as compared with BSA-treated cultures (Fig.4B). As reported previously (Sagomonyants et al. 2015), FGF2-treated cultures also showed transient increases in the expression *Dmp1* and *osteocalcin* that are expressed by both odontoblasts and osteoblasts (Fig. 4C,

Table. Effect of FGF2 on the Proliferation of Pulp and αSMA Cells In Vitro.

A.

	% αSMA-GFP+		% αSMA-GFP–	
	BSA	FGF2	BSA	FGF2
24h	94.72 ± 1.02	96.97 ± 0.8*	5.27 ± 1.02	3.05 ± 0.8
48h	93.6 ± 1.06	95.75 ± 0.8*	6.72 ± 1.02	4.3 ± 0.7
72h	88.75 ± 2.2	94.27 ± 1.15*	11.25 ± 2.3	5.72 ± 1.5*
96h	71.6 ± 0.4	81.53 ± 1.98*	28.4 ± 0.75	18.46 ± 1.7*

B.

	%EdU+		%EdU–	
	BSA	FGF2	BSA	FGF2
24h	20.6 ± 1.36	33.87 ± 0.2*	79.4 ± 1.35	66.12 ± 0.2*
48h	9.82 ± 0.32	15.53 ± 0.6*	90.17 ± 0.3	84.46 ± 0.6*
72h	18.9 ± 1.03	22.17 ± 1.06*	81.1 ± 1.03	77.82 ± 1.06*
96h	14.92 ± 1.8	10.6 ± 1.43	85.07 ± 1.81	89.4 ± 1.43

C.

	% αSMA-GFP+/EdU+		% αSMA-GFP+/EdU–	
	BSA	FGF2	BSA	FGF2
24h	18.82 ± 1.5	31.82 ± 0.4*	77.9 ± 1.85	65.15 ± 0.9*
48h	8.17 ± 0.1	13.42 ± 1.3*	85.42 ± 0.9	82.32 ± 1.4
72h	15.9 ± 1.5	18.8 ± 0.2*	72.85 ± 3.1	75.47 ± 1.1
96h	7.56 ± 1.7	4.26 ± 0.9*	64.03 ± 2.16	77.26 ± 2.9*

Primary pulp cultures from αSMA-GFP transgenic mice were treated with bovine serum albumin (BSA) or 20 ng/mL of fibroblast growth factor 2 (FGF2) starting on day 3. Cells were processed for staining with EdU and fluorescence-activated cell sorting analysis at 24 to 96 h after treatment. Note the significant increases in the percentage of αSMA-GFP+ (**A**), Edu+ (**B**), and αSMA-GFP+/Edu+ (**C**) cells at all time points in FGF2-treated cultures as compared with BSA-treated cultures. Results represent the mean ± SEM in at least 3 independent experiments.
*$P \leq 0.05$ relative to control at each time point.

D). However, there were no differences in the levels of *Dmp1* and *Osteocalcin* in FGF2-and BSA-treated cultures at days 14 and 17 (Fig. 4C, D). Together, these observations indicated that early treatment with FGF2 accelerated and promoted the differentiation of odontoblasts expressing high levels of *Dspp* and inhibited the differentiation of osteoblasts expressing *Bsp*.

Discussion

Numerous studies have shown that application of biologically active materials to the amputated pulp resulted in the formation of calcified bridge/reparative dentin (Tziafas 2004). The reparative dentin in these studies in most (but not all) cases consisted of the formation of osteodentin, which is porous and more fragile than that of dentin and unable to provide the necessary barrier effect to protect the pulp from exogenous destructive stimuli (Tziafas 2004).

In the present study, we showed that limited and early exposure of pulp cells to FGF2 resulted in proliferative expansion of αSMA-tdTomato+perivascular cells. Our lineage tracing experiments showed that FGF2 accelerated and promoted the differentiation of a second generation of *Dspp*+ odontoblasts from αSMA-tdTomato+ cells and inhibited their differentiation into *Bsp*+ osteoblasts.

The promotion of odontoblast differentiation and the inhibition of osteoblast differentiation by αSMA-tdTomato+ cells in FGF2-treated pulps in our study suggest that FGF signaling may play a significant role in fate determination of αSMA-td Tomato+ cells in the dental pulp. These changes are most likely related to differences in the response to FGFR/ERK1/2 signaling by early odontoprogenitors versus osteoprogenitors. Our previous in vitro studies showed that activation of FGFR/Erk1/2 in early odontoprogenitors resulted in enhanced odontoblast differentiation (Sagomonyants et al. 2015, 2017). Previous studies have shown that in early osteoprogenitors, FGFR/Erk1/2 primarily leads to increased cell proliferation but not differentiation (Choi et al. 2008).

The differences in response to FGF signaling by odontoprogenitors and osteoprogenitors in our studies are supported by previous studies (James et al. 2006; Li et al. 2011; Liu et al. 2013). Studies in the Runx2 null mutants showed that in teeth, *Runx2*-dependent genes are activated by FGF, whereas in bone, *Runx2*-dependent genes are activated by BMP (James et al. 2006). Also, in dental mesenchyme, FGF by inhibiting Wnt/β-catenin signaling maintains the odontogenic fate of dental mesenchyme (Liu et al. 2013). Elevated levels of Wnt/β-catenin in dental mesenchyme resulted in loss of odontogenic fate and replacement of dentin by bonelike structures (Li et al. 2011; Liu et al. 2013).

Althoughit is not currently known if individual αSMA-tdTomato+ cells are multi- or bipotent, recent clonal genetic tracing experiments in mice incisors demonstrated that an individual MSC is at least bipotential, and their differentiation fate is dependent on the extrinsic signals (Krivanek et al. 2017).

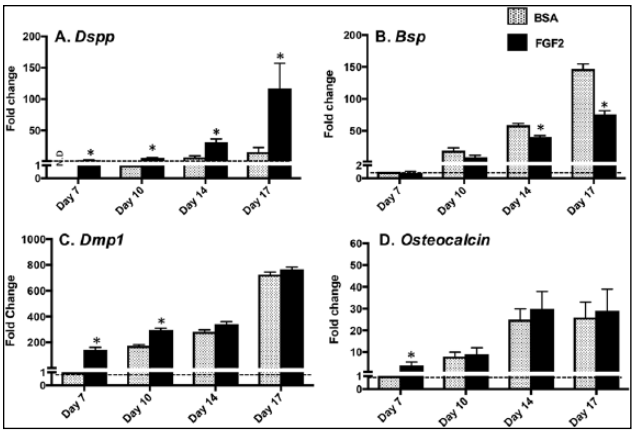

Figure 4. Effects of fibroblast growth factor (FGF2) on differentiation of primary pulp cells in vitro.Histograms showing the expression of *Dspp* (**A**), *Bsp* (**B**), *Dmp1* (**C**), and *Osteoclacin* (**D**) in primary dental pulp cultures from nontransgenic mice after exposure to FGF2 and bovine serum albumin (BSA) between days 3 and 7. Expression of *Dspp* was normalized to that in BSA-treated cultures at day 10, which is arbitrarily set to 1 and is indicated by the dashed line. Expression of *Bsp*, *Dmp1*, and *Osteoclacin* were normalized to that in BSA-treated cultures at day 7, which is arbitrarily set to 1 and is indicated by the dashed line. Results in all histograms represent mean ± SEM in at least 3 to 5 independent experiments; $P \leq 0.05$ relative to BSA control at each time point.

Our observations on the effects of limited and early release of FGF2 on reparative dentinogenesis are different from previous reported effects of FGF2 from gelatin hydrogels (Kikuchi et al. 2007; Ishimatsu et al. 2009; Kitamura et al. 2012). These studies showed that continual release of FGF2 resulted in the formation of dentin-like particles and/or osteodentin depending on the dose of FGF2 (Kikuchi et al. 2007; Ishimatsu et al. 2009; Kitamura et al. 2012). Cells lining these particles and the calcified bridge were shown to express DMP1 but not Nestin, a marker for mature anf differentiated odontoblasts. Our studies provide further evidence that the absence of fully differentiated odontoblasts after continual release of FGF2 is related to stage-specific effects of FGF2 on cells in odontoblast lineage (Sagomonyants and Mina 2014; Sagomonyants et al. 2015, 2017).

The calcified matrix/reparative dentin formed in our study that is devoid of osteoblasts is similar to the calcified matrix/reparative dentin formed in animal models with elevated levels of Wnt/β-catenin signaling (Hunter et al. 2015; Ishimoto et al. 2015; Neves et al. 2017). Lineage tracing experiments showed the contribution of Axin2-expressing cells in dental pulp to odontoblast-like cells secreting calcified matrix/reparative dentin in response to elevated levels of Wnt/β-catenin signaling (Babb et al. 2017). The similarities in the effects of early and limited exposure of dental pulp to FGF and elevated levels of Wnt signaling on dental pulp suggest possible interactions between FGF and Wnt signaling in reparative dentinogenesis and dentin regeneration. Genetic and functional evidence has shown that the interactions between FGF and Wnt/β-catenin signaling control MSC fate and differentiation (Ornitz and Marie 2002, 2015).

Taken together, our observations support the key roles of FGF signaling in fate determination of perivascular cells expressing αSMA, which leads to the formation of reparative dentin that is devoid of osteoblasts.

Author Contributions

I. Vidovic-Zdrilic, I. Kalajzic, D.J. Mooney, M. Mina, contributed to conception, design, data acquisition, analysis, and interpretation, drafted and critically revised the manuscript; K.H. Vining, A. Vijaykumar, contributed to conception, design, data acquisition, analysis, and interpretation, drafted the manuscript. All authors gave final approval and agree to be accountable for all aspects of the work.

Acknowledgments

The authors thank all individuals who provided reagents, valuable input, and technical assistance in various aspects of this study, including Dr. David Rowe, Mrs. Barbara Rodgers, and members of the Molecular Core Facility and Flow Cytometry Facility at the University of Connecticut Health Center. This work was supported by grants R01-DE016689 (M.M.), R90-DE022526 (K.H.V.), and K08DE025292 (K.H.V.) from the National Institutes of Health (National Institute of Dental and Craniofacial Research). The authors declare no potential conflicts of interest with respect to the authorship and/or publication of this article.

ORCID iD

K.H. Vining https://orcid.org/0000-0002-4009-879X

References

Babb R, Chandrasekaran D, Carvalho Moreno Neves V, Sharpe PT. 2017. Axin2-expressing cells differentiate into reparative odontoblasts via autocrine Wnt/beta-catenin signaling in response to tooth damage. Sci Rep. 7(1):3102.

Balic A, Aguila HL, Caimano MJ, Francone VP, Mina M. 2010. Characterization of stem and progenitor cells in the dental pulp of erupted and unerupted murine molars. Bone. 46(6):1639–1651.

Braut A, Kollar EJ, Mina M. 2003. Analysis of the odontogenic and osteogenic potentials of dental pulp in vivo using a Col1a1-2.3-GFP transgene. Int J Dev Biol. 47(4):281-292.

Choi SC, Kim SJ, Choi JH, Park CY, Shim WJ, Lim DS. 2008. Fibroblast growth factor-2 and -4 promote the proliferation of bone marrow mesenchymal stem cells by the activation of the PI3K-Akt and ERK1/2 signaling pathways. Stem Cells Dev. 17(4):725–736.

Feng J, Mantesso A, De Bari C, Nishiyama A, Sharpe PT. 2011. Dual origin of mesenchymal stem cells contributing to organ growth and repair. Proc Natl Acad Sci USA. 108(16):6503–6508.

Frozoni M, Balic A, Sagomonyants K, Zaia AA, Line SR, Mina M. 2012. A feasibility study for the analysis of reparative dentinogenesis in pOBCol3.6GFPtpz transgenic mice. Int Endod J. 45(10):907–914.

Hunter DJ, Bardet C, Mouraret S, Liu B, Singh G, Sadoine J, Dhamdhere G, Smith A, Tran XV, Joy A, et al. 2015. Wnt acts as a prosurvival signal to enhance dentin regeneration. J Bone Miner Res. 30(7):1150–1159.

Ishimatsu H, Kitamura C, Morotomi T, Tabata Y, Nishihara T, Chen KK, Terashita M. 2009. Formation of dentinal bridge on surface of regenerated dental pulp in dentin defects by controlled release of fibroblast growth factor-2 from gelatin hydrogels. J Endod. 35(6):858–865.

Ishimoto K, Hayano S, Yanagita T, Kurosaka H, Kawanabe N, Itoh S, Ono M, Kuboki T, Kamioka H, Yamashiro T. 2015. Topical application of lithium chloride on the pulp induces dentin regeneration. PLoS One. 10(3):e0121938.

James MJ, Jarvinen E, Wang XP, Thesleff I. 2006. Different roles of Runx2 during early neural crest-derived bone and tooth development. J Bone Miner Res. 21(7):1034–1044.

Kaukua N, Shahidi MK, Konstantinidou C, Dyachuk V, Kaucka M, Furlan A, An Z, Wang L, Hultman I, Ahrlund-Richter L, et al. 2014. Glial origin of mesenchymal stem cells in a tooth model system. Nature. 513(7519): 551–554.

Kikuchi N, Kitamura C, Morotomi T, Inuyama Y, Ishimatsu H, Tabata Y, Nishihara T, Terashita M. 2007. Formation of dentin-like particles in dentin defects above exposed pulp by controlled release of fibroblast growth factor 2 from gelatin hydrogels. J Endod. 33(10):1198–1202.

Kitamura C, Nishihara T, Terashita M, Tabata Y, Washio A. 2012. Local regeneration of dentin-pulp complex using controlled release of FGF-2 and naturally derived sponge-like scaffolds. Int J Dent. 2012:190561.

Krivanek J, Adameyko I, Fried K. 2017. Heterogeneity and developmental connections between cell types inhabiting teeth. Front Physiol. 8:376.

Li J, Huang X, Xu X, Mayo J, Bringas P Jr, Jiang R, Wang S, Chai Y. 2011. SMAD4-mediated WNT signaling controls the fate of cranial neural crest cells during tooth morphogenesis. Development. 138(10):1977–1989.

Liu C, Gu S, Sun C, Ye W, Song Z, Zhang Y, Chen Y. 2013. FGF signaling sustains the odontogenic fate of dental mesenchyme by suppressing beta-catenin signaling. Development. 140(21):4375–4385.

Neves VC, Babb R, Chandrasekaran D, Sharpe PT. 2017. Promotion of natural tooth repair by small molecule GSK3 antagonists. Sci Rep. 7:39654.

Ornitz DM, Marie PJ. 2002. FGF signaling pathways in endochondral and intramembranous bone development and human genetic disease. Genes Dev. 16(12):1446–1465.

Ornitz DM, Marie PJ. 2015. Fibroblast growth factor signaling in skeletal development and disease. Genes Dev. 29(14):1463–1486.

Roguljic H, Matthews BG, Yang W, Cvija H, Mina M, Kalajzic I. 2013. In vivo identification of periodontal progenitor cells. J Dent Res. 92(8): 709–715.

Sagomonyants K, Kalajzic I, Maye P, Mina M. 2015. Enhanced dentinogenesis of pulp progenitors by early exposure to FGF2. J Dent Res. 94(11): 1582–1590.

Sagomonyants K, Kalajzic I, Maye P, Mina M. 2017. FGF signaling prevents the terminal differentiation of odontoblasts. J Dent Res. 96(6):663–670.

Sagomonyants K, Mina M. 2014. Stage-specific effects of fibroblast growth factor 2 on the differentiation of dental pulp cells. Cells Tissues Organs. 199(5–6):311–328.

Sloan AJ, Smith AJ. 2007. Stem cells and the dental pulp: potential roles in dentine regeneration and repair. Oral Dis. 13(2):151–157.

Sloan AJ, Waddington RJ. 2009. Dental pulp stem cells: what, where, how? Int J Paediatr Dent. 19(1):61–70.

Tziafas D. 2004. The future role of a molecular approach to pulp-dentinal regeneration. Caries Res. 38(3):314–320.

Vidovic I, Banerjee A, Fatahi R, Matthews BG, Dyment NA, Kalajzic I, Mina M. 2017. αSMA-expressing perivascular cells represent dental pulp progenitors in vivo. J Dent Res. 96(3):323–330.

Zhao H, Feng J, Seidel K, Shi S, Klein O, Sharpe P, Chai Y. 2014. Secretion of Shh by a neurovascular bundle niche supports mesenchymal stem cell homeostasis in the adult mouse incisor. Cell Stem Cell. 14(2):160–173.